

Absorption of carbon dioxide by the absorbent composed of piperazine and 2-amino-2-methyl-1-propanol in PVDF membrane contactor

Su-Hsia Lin^{a,*}, Pen-Chi Chiang^b, Chun-Fan Hsieh^c, Meng-Hui Li^c, Kuo-Lun Tung^{c,d}

^aDepartment of Chemical and Material Engineering, Nanya Institute of Technology, Chung-Li 32091, Taiwan

^bGraduate Institute of Environmental Engineering, National Taiwan University, Taipei 106, Taiwan

^cDepartment of Chemical Engineering, Chung Yuan Christian University, Chung-Li 32023, Taiwan

^dR&D Center for Membrane Technology, Chung Yuan University, Chung-Li 32033, Taiwan

Received 3 October 2007; accepted 26 November 2007

Abstract

This paper tests the performance of microporous polyvinylidene fluoride (PVDF) hollow fiber in a gas absorption membrane process (GAM) using the aqueous solutions of piperazine (PZ) and 2-amino-2-methyl-1-propanol (AMP). Experiments were conducted at various gas flow rates, liquid flow rates and absorbent concentrations. Experimental results showed that wetting ratio was about 0.036% when used with the aqueous alkanolamine solutions, while that was 0.39% with aqueous piperazine solutions. The CO₂ absorption rates increased with increasing both liquid and gas flow rates at $N_{Re} < 20$. The increase of the PZ concentration showed an increase of absorption rate of CO₂. The CO₂ absorption rate was much enhanced by the addition of PZ promoter. The resistance of membrane was predominated as using a low reactivity absorbent and can be neglected as using absorbent of AMP aqueous solution. The resistance of gas-film diffusion was dominated as using the mixed absorbents of AMP and PZ. An increase of PZ concentration, the resistance of liquid-film diffusion decreased but resistance of gas-film increased. Overall, GAM systems were shown to be an effective technology for absorbing CO₂ from simulated flue gas streams, but the viscosity and solvent–membrane relationship were critical factors that can significantly affect system performance.

© 2008 Taiwan Institute of Chemical Engineers. Published by Elsevier B.V. All rights reserved.

Keywords: Carbon dioxide absorption; Piperazine; 2-amino-2-methyl-1-propanol; PVDF hollow fiber; Membrane contactor; Wetting

1. Introduction

Carbon dioxide has been proven to be the largest contribution of greenhouse gases, increasing of the earth's surface temperature. And it is reported that half of the CO₂ emission is produced by power plants using fossil fuels (Desideri and Paolucci, 1999). Therefore, the development of a separation process is highly needed to remove and to recover the CO₂ from the places generating CO₂ gas. In general, the bubble columns, packed towers, venturi scrubber, sieve trays can be used to remove the CO₂. The commercial process widely known for CO₂ separation is the packed column system, but new technology is required for this because of disadvantages of

the packed column system, such as flooding, channeling, large-scale equipment, etc. Gas absorption membrane (GAM) process was considered as an alternative to recovery of CO₂ from waste gas streams. Hollow fiber membrane contactor (HFMC) offers a much larger contact area per unit volume compared to tray and packed columns, which has the advantages of no flooding, entrainment, and foaming restrictions on operation flow rates (Gabelman and Hwang, 1999; Rangwala, 1996).

The mass transfer resistances of gas, membrane, and liquid phases limit the CO₂ absorption rate in the membrane contactor module. Although the interfacial area of the membrane is greater than conventional absorbers, the increase of its additional membrane resistance can cause a decrease in the mass transfer capacity of the membrane (Li and Chen, 2005). Therefore, to minimize the membrane resistance plays an important part in the gas absorption

* Corresponding author. Fax: +886 3 4652040.

E-mail address: sslin@nanya.edu.tw (S.-H. Lin).

Nomenclature

a	gas–liquid contact area (m^2/m^3)
d_i, d_o	inside and out side diameter of the fiber, respectively (m)
D_e	average of diffusivity defined as Eq. (7) (m^2/s)
D_g	diffusivity of CO_2 in gas phase (m^2/s)
D_k	Knudsen diffusivity of CO_2 (m^2/s)
D_L	diffusivity of RNH_2 in liquid phase (m^2/s)
E	enhancement factor
H_e	Henry's law constant of CO_2 ($\text{m}^3 \text{kPa}/\text{kmol}$)
J_{CO_2}	flux of CO_2 ($\text{kmol}/\text{m}^2 \text{s}$)
k_g	gas phase mass transfer coefficient ($\text{kmol}/\text{s m}^2 \text{kPa}$)
k_L	liquid-film mass transfer coefficient (m/s)
k_m	membrane mass transfer coefficient (m/s)
k_{OH}^*	reaction rate of CO_2 hydration
k_{ov}	overall pseudo first-order reaction rate constant (1/s)
K_L	overall liquid phase mass transfer coefficient (1/s)
L	fiber length (cm)
n	number of fibers
P	overall pressure (kPa)
P_{BM}	log–mean partial pressure of inert (kPa)
P_g, P_i, P_m	CO_2 partial pressures in the bulk gas phase, membrane–liquid interface, and gas–membrane interface, respectively (kPa)
P_M	log–mean partial pressure of CO_2 (kPa)
r_{ov}	overall pseudo first-order reaction rate ($\text{kmol}/\text{m}^3 \text{s}$)
R	gas constant ($\text{kJ}/\text{mol K}$)
R_{CO_2}	absorption rate of reaction of CO_2 ($\text{kmol}/\text{m}^3 \text{s}$)
R_M, R_G, R_L	were represented as the resistances of membrane, gas-film and liquid-film diffusion
T	absolute temperature (K)
v_g	velocity of gas phase (m/s)
v_L	velocity of liquid phase (m/s)
X	average fractional depth of penetration of liquid into pores
<i>Greek symbols</i>	
$\Delta_m, \Delta_G, \Delta_L$	were represented as the fractional resistances of membrane, gas-film and liquid-film diffusion to overall resistances defined as Eq. (11).
β	penetration ratio of liquid
ε	porosity of membrane
γ_H	hydraulic irradius (m)
μ	viscosity of liquid (m Pa s)
μ_g	viscosity of gas (Pa s)
ν_L	velocity of liquid (m/s)
ρ	density of gas phase (kg/m^3)
τ	fiber tortuosity

process by using a polymeric membrane contactor. The success of this technology is highly dependent on the wetting relationship between the membrane and liquid solvent used in the system.

The alkanolamine group is mainly used as absorbent for removal of the CO_2 due to its high reaction rate. A wide variety of alkanolamines has been studied in the literatures, such as monoethanolamine (MEA), *N*-methyldiethanolamine (MDEA), diglycolamine (DGA), di-2-propanolamine (DIPA), and 2-amino-2-methyl-1-propanol (AMP) (Li and Lie, 1994; Song et al., 1996; Versteeg and van Swaaij, 1988). Piperazine has a higher reaction than primary alkanolamine like MEA because of its cyclic and diamine nature, considered as a promoter for methyl diethanolamine (Bishnoi and Rochelle, 2000; Xu et al., 1992, 1998). The sterically hindered amines such as AMP also have higher cyclic capacities of CO_2 than conventional primary and secondary amines such as MEA, diethanolamine (DEA), and diisopropanolamine (DIPA) and more appreciable rates of absorption (Satori and Savage, 1983).

However, the properties of these sterically hindered amines are unflavored mainly due to the instability of carbamate (Alper, 1990; Chakraborty et al., 1986; Saha et al., 1995). Recently, it has been shown that a solution of two or more amines improves the absorption rate and reduces the solvent regeneration energy (Chakravarty et al., 1985; Seo and Hong, 1996). Appl et al. (1982) reported that piperazine would be more effective than the conventional absorption accelerators. Xu et al. (1992) investigated the kinetics of CO_2 absorption in activated MDEA solutions that contained piperazine as an activator. Xiao et al. (2000) investigated the kinetics of CO_2 into aqueous solutions of AMP with the small addition of MEA. They suggested a hybrid reaction model, a first-order reaction for MEA, and a zwitterions mechanism for AMP to interpret the kinetic data. Here the aqueous mixtures solutions of piperazine and AMP were chosen as a novel absorbent in this study.

Although there are some literatures that investigated the CO_2 absorption in hollow fiber. Yeon et al. (2003) have ever investigated the CO_2 absorption in PVDF and PTFE hollow fiber membrane using single absorbent (MEA). Wang et al. (2004) studied the CO_2 capture by three typical amines solutions (MDEA, AMP and DEA) in hollow fiber membrane contactors. Yeon et al. (2004) have ever studied the CO_2 absorption rate using the mixed absorbent of PZ and TEA. However, the characteristics and efficiency of the mixed absorbents on membrane were not clear. In this study, we experimentally investigated the CO_2 absorption rate in a PVDF membrane contactor using a mixture solution of PZ and AMP. The influence of liquid and gas flow rates on CO_2 absorption rate and interfacial area were investigated. Besides, the effects of absorbents on wetting of membrane and the resistances of mass transfer were also discussed.

2. Kinetic theory

2.1. Film model

The mass transfer between gas and liquid through the hollow fiber membrane contactor occurs in three parts; gas film,

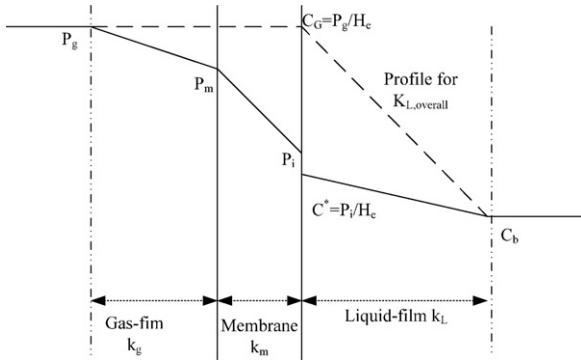


Fig. 1. Film model for mass transfer across an ideal non-wetted membrane.

membrane, and liquid film (Yeon *et al.*, 2003) as shown in Fig. 1. The CO₂ flux per unit fiber length at any cross-section, J can be expressed by Eq. (1).

$$J(n\pi d_i) = K_L(n\pi d_i) \left(\frac{P_g}{H_e} \right) = k_g(n\pi d_i)(P_g - P_m) \\ = \left(\frac{k_m}{RT} \right) (n\pi d_i)(P_m - P_i) = k_L E(n\pi d_i) \left(\frac{P_i}{H_e} \right) \quad (1)$$

where k_L , k_m , and k_g indicate the mass transfer coefficients (m/s) of the liquid phase, membrane, and gas phase, respectively, K_L is overall liquid phase mass transfer coefficient, n is the number of the fiber; d_i and d_o are inside and outside diameter of the fiber; P_g , P_i , and P_m , are CO₂ partial pressures in the bulk gas phase, membrane–liquid interface, and gas–membrane interface, respectively (kPa); H_e is the Henry's constant (m³ kPa/kmol); and E is enhancement factor. The overall resistance in liquid phase mass transfer through the porous hollow fiber membrane contactor can be expressed as the following Eq. (2) (Kreulen *et al.*, 1993).

$$\frac{1}{K_L} = \left(\frac{d_i}{d_o k_g} \right) \left(\frac{1}{H_e} \right) + \left(\frac{d_i}{d_o k_m} \right) \left(\frac{RT}{H_e} \right) + \frac{1}{E k_L} \quad (2)$$

If film model for mass transfer is across an ideal non-wetted membrane (Yeon *et al.*, 2003). The overall mass transfer coefficient, K_L can be obtained by Eq. (3).

$$r_{ov} = k_{ov}[\text{CO}_2] \\ = k_{2,\text{PZ}}[\text{CO}_2][\text{PZ}] + k_{\text{OH}^-}^*[\text{CO}_2][\text{OH}^-] + \frac{[\text{AMP}][\text{CO}_2]}{(1/k_{2,\text{ANP}} + k_{2,\text{AMP}}k_{\text{H}_2\text{O}}[\text{OH}^-]/k_{-1} + k_{2,\text{AMP}}K_{\text{PZ}}[\text{PZ}]/k_{-1} + k_{2,\text{AMP}}k_{\text{AMP}}[\text{AMP}]/k_{-1})} \quad (9)$$

$$K_L a = \left(\frac{R}{\Delta P_M / H_e} \right) \quad (3)$$

where R is CO₂ absorption rate (kmol/m³ s) per unit volume of the contactor.

2.2. Individual gas-film mass transfer coefficients

The individual mass transfer coefficient of liquid phase k_L can be predicted using the equation followed (Nii and Takeuchi, 1994; Rangwala, 1996):

$$\frac{k_L d_i}{D_L} = 1.62 \left(\frac{d_i^2 v_L}{LD_L} \right)^{1/3} \quad (4)$$

The individual mass transfer coefficient of gas phase used the proposed correlation as followed (Gilliland and Sherwood, 1934):

$$\frac{k_g d_e}{D_g} = 0.023 \left(\frac{4\gamma_H \rho v_g}{\mu_g} \right)^{0.83} \left(\frac{\mu_g}{D_g \rho} \right)^{0.44} \quad (5)$$

The membrane mass transfer coefficient is predicted using the Eq. (6). Here the effective diffusivity as calculated from the harmonic mean is showed in Eq. (7).

$$k_m = \frac{2D_e \varepsilon}{\tau d_i \ln(d_o/d_i)} \quad (6)$$

$$D_e^{-1} = D_k^{-1} + D_g^{-1} \quad (7)$$

Using the values in Eq. (6) for the fiber used in the hollow fiber module, $k_{m,\text{gas filled}}$ is estimated as 2.69×10^{-3} m/s. In the case of liquid filled pores, the effective diffusivity is similar to that of CO₂ in the solution (1.49×10^{-9} m²/s), and $k_{m,\text{liquid filled}}$ is about 2.62×10^{-7} m/s. If the pores are partial filled with liquid, then k_m was of the average fractional depth of liquid penetration β can be calculated from

$$\frac{1}{k_m} = \frac{\beta}{k_{m,\text{liquid filled}}} + \frac{(1-\beta)}{k_{m,\text{gas filled}}} \quad (8)$$

2.3. Interfacial reaction rate for CO₂ absorption into PZ + AMP + H₂O

For the absorption of CO₂ into PZ + AMP + H₂O, the overall CO₂ reaction rate can then be expressed as follows (Sun *et al.*, 2005):

where $k_{2,\text{AMP}}$ is the reaction rate constant for formation of a zwitterions from CO₂ and AMP, k_{-1} is the reaction rate constant for the reverse reaction of the zwitterion, $k_{\text{H}_2\text{O}}$, K_{OH^-} , k_{PZ} , k_{AMP} are the reaction rate constants for subsequent removal proton reaction from a zwitterions by bases: H₂O, OH⁻, PZ and AMP, respectively.

Here, the apparent reaction rate constant, k_{app} , is defined as followed

$$k_{app} = k_{ov} - k_{OH^-}^* [OH^-] = k_{2,PZ} [PZ] + \frac{[AMP]}{(1/k_{2,ANP} + k_{2,AMP} k_{H_2O} [OH^-] / k_{-1} + k_{2,AMP} K_{PZ} [PZ] / k_{-1} + k_{2,AMP} k_{AMP} [AMP] / k_{-1})} \quad (10)$$

3. Experimental

3.1. Materials

Piperazine and AMP were purchased from Aldrich Chemicals. The membrane contactor used as CO₂ absorbers in this study is the polyvinylidene fluoride (PVDF) hollow fibers supported from Pall Co. (UMP-0047R). Details of the hollow fiber were listed in Table 1. Deionized water was used. All chemicals were used without any further purification.

3.2. Absorption of carbon dioxide

The experimental set-up for CO₂ removal and recovery was shown in Fig. 2. The gas containing 1–15% of CO₂ (balance N₂) was passed upstream in the tube side of the membrane module, and the absorbent was supplied downstream in the shell side. The absorbents used in this system are mixed solutions of piperazine 0.1–0.4 M, and 1 M AMP. The gas flow rate was changed at the range of 100–600 cm³/min, and the liquid flow rate was changed at the range of 100–400 cm³/min. The solution was reused after the CO₂ dissolved in the solution was totally stripped in the desorption tower connected with the reboiler. The pressure difference of the liquid phase and the gas phase was kept in the range of 2–5 psig by a needle valve to form the stable gas–liquid interface in the membrane module. The gases coming from the absorption were sampled and analyzed by TCD-GC (GC-14B; Shimadzu) at steady state (about 15–20 min).

4. Results and discussion

4.1. Effects of flow rate on specific surface area

The objective of this section was to investigate the effective contact areas of this module under the studied conditions. The N₂–CO₂–H₂O system was used due to the CO₂ absorption rate is low by H₂O solution. The absorption rates of CO₂ using water

Table 1
Characteristics of hollow fiber module (UMP-0047R)

Module o.d. (mm)	16
Shell i.d. (mm)	14
Fiber o.d. (mm)	2.2
Fiber i.d. (mm)	1.4
Fiber length (cm)	31.4
Number of fibers	21
Average pore size (μm)	0.2
Fiber porosity, ε (%)	50
Surface area (nominal m ²)	0.02

at 30 °C at various gas and liquid flow rate are shown in Table 2. It can be seen that the absorption rates in Table 2 are almost independent of gas flow rates, revealing that the resistance of gas-film diffusion is insignificant compared to that of liquid-film diffusion in N₂–CO₂–H₂O system. Rangwala (1996) and Yang and Cussler (1986) have ever reported similar trend for air–CO₂–H₂O system. The pores will be gas-filled due to the fact that PVDF membrane is hydrophobic. The gas-filled membrane results in a neglect resistance of diffusion in pores compared to that of liquid-film. Thus, the measured overall K_L will be nearly equal to k_L in Eq. (2). The effective gas–liquid contact area per volume can be calculated from the measured values of $K_L a$ from Eq. (3) (Rangwala, 1996). The calculated effective gas–liquid contact areas are below the geometrical areas (nominal contact areas = 0.02 m²) shown as Fig. 3. As shown in Fig. 3, the effective gas–liquid contact areas per volume are influenced on the fluid flow rates. These results indicated that the greater effective contact areas per volume will be obtained at higher fluid velocities. So we suggested that the fluid flow rate was operated at the condition of $N_{Re} > 15$ to prevent losing the effective specific contact areas.

4.2. Effect of operational parameters on absorption rate

Figs. 4–6 showed the CO₂ absorption rate in PVDF membrane modules using the mixed solution of AMP and PZ as absorbent. The CO₂ absorption rate increased with both gas and liquid flow rates initially, and then reached a plateau shown as Figs. 4 and 5. It was because that an increase of

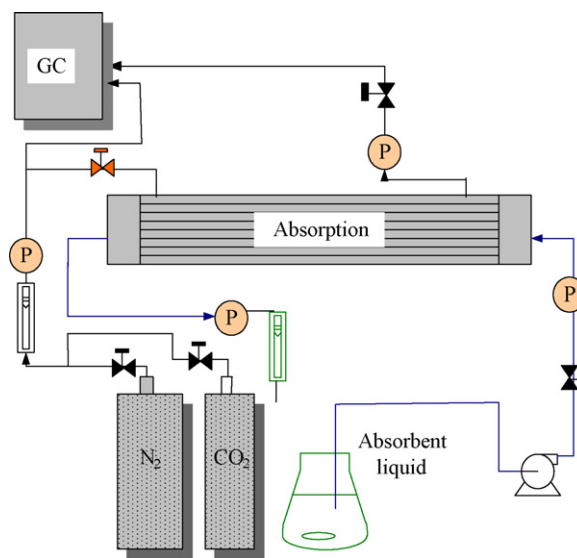


Fig. 2. Experimental set-up.

Table 2
Absorption rate of CO₂ with H₂O in hollow fiber

Q_G (cm ³ /min)	Q_L (cm ³ /min)	R (kmol/m ³ s)
357	100	8.4×10^{-7}
	200	1.1×10^{-6}
	300	1.2×10^{-6}
	400	1.4×10^{-6}
429	100	8.3×10^{-7}
	200	9.7×10^{-7}
	300	1.2×10^{-6}
	400	1.4×10^{-6}
499	100	8.5×10^{-7}
	200	9.9×10^{-7}
	300	1.2×10^{-6}
	400	1.4×10^{-6}

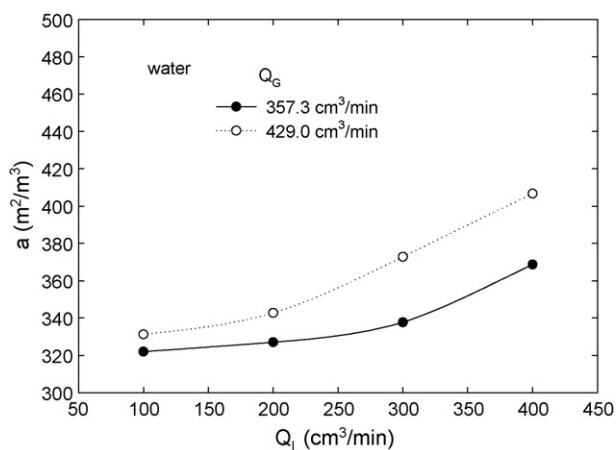


Fig. 3. The specific area at different fluid flow rates of hollow fiber module.

velocity in hollow fiber can reduce the resistance of stagnant-layer diffusion under laminar flow. Yeon *et al.* have ever investigated the CO₂ absorption in PVDF and PTFE hollow fiber membrane using single absorbent (MEA) (Yeon *et al.*, 2003). They also found the similar behavior that the CO₂ flux increased with an increase of liquid velocity and that increased initially with an increase of gas velocity. Wang *et al.* (2004)

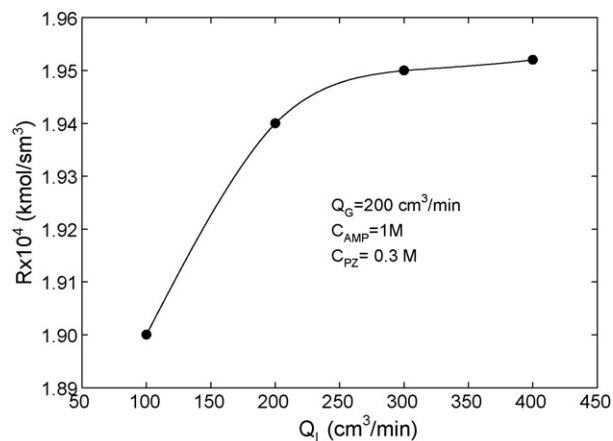


Fig. 4. CO₂ absorption rates at various liquid flow rate in HFMC.

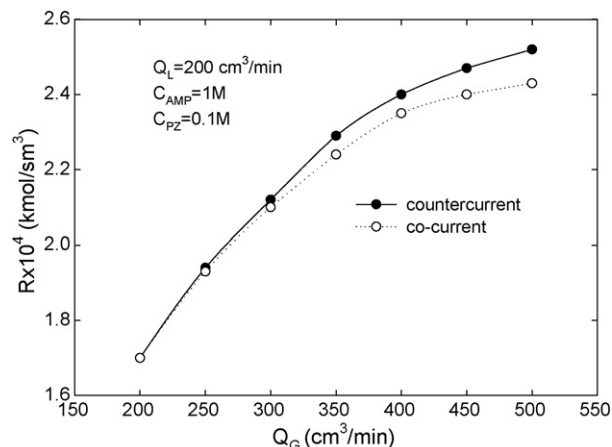


Fig. 5. CO₂ absorption rates at various gas flow rate in HFMC.

studied the CO₂ capture by three typical amines solutions in hollow fiber membrane contactors. They reported that CO₂ absorption flux in MDEA solution is virtually unaffected by the liquid flow velocity. However, that for both AMP and DEA solutions, the CO₂ absorption flux increased with an increase in liquid flow velocity. It was due to that the reaction rate of CO₂ with MDEA was much slower than that of AMP and DEA (Wang *et al.*, 2004).

As shown in Fig. 6, the CO₂ absorption rate was 1.8×10^{-4} kmol/m³ s with the AMP (1 M) solution and that was enhanced to 2.4×10^{-4} kmol/m³ s by the addition of 0.1 M PZ promoter at $Q_G = 400$ cm³/min and $Q_L = 200$ cm³/min. Although the CO₂ absorption rate was already reaching 1.3×10^{-4} kmol/m³ s with only PZ (0.1 M) solution, the PZ was unflavored used individually due to its instability of carbamate. One reason for choosing the mixture of AMP and PZ was that AMP has higher cyclic capacities of CO₂ than conventional primary and secondary amines.

Fig. 7 showed the effect of PZ concentration on the CO₂ absorption rate. It can be seen the CO₂ absorption rate increased with increasing PZ concentration first and then reached a maximum. It was unusual to find that the CO₂ absorption rate drop beyond 0.3 M PZ concentration. It was likely that the

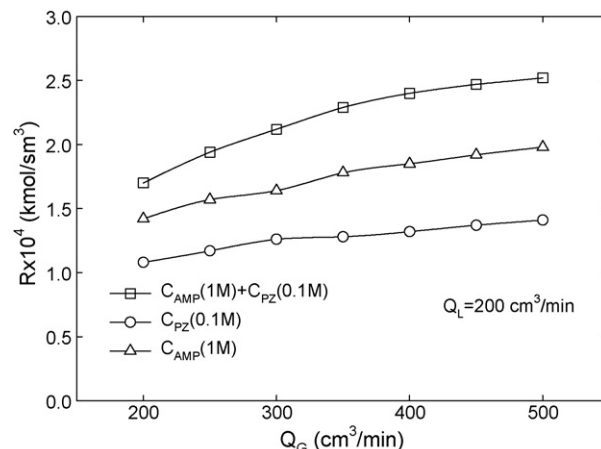
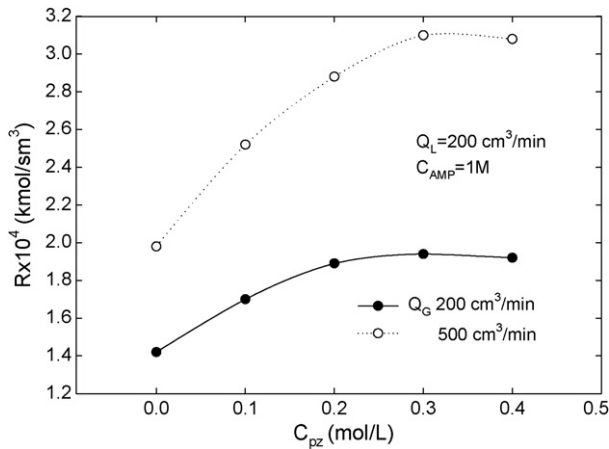


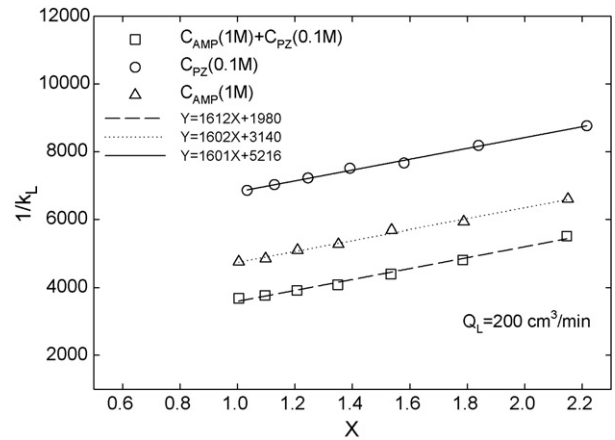
Fig. 6. CO₂ absorption rates at various absorbents in HFMC.

Fig. 7. CO₂ absorption rates at different PZ concentration in HFMC.

higher viscosity of the aqueous solution (1 M AMP + 0.4 M PZ) reduced the CO₂ absorption rate. The study using ethanolamine mixed with PZ as absorbent was found by *Yeon et al.* (2004). They investigated the CO₂ absorption rate using the mixed absorbent of PZ and TEA and reported that the CO₂ absorption rate was 8 times higher than that of the TEA alone. They thought that these results were caused by the difference of the reaction mechanism between PZ and TEA (*Yeon et al.*, 2004). Because it was hard to compare the CO₂ absorption rate with two kinds of mixed absorbents with different pore size PVDF membrane modules. We also tested the CO₂ absorption with the mixed absorbents of TEA (1 M) and PZ (0.1 M). The CO₂ absorption rate using TEA (1 M) and PZ (0.1 M) was found to be 1.3×10^{-4} kmol/m³ s. So in our system, the CO₂ absorption rate by absorbents of AMP (1 M) and PZ (0.1 M) ($R = 2.52 \times 10^{-4}$ kmol/m³ s) was better than that of by TEA (1 M) and PZ (0.1 M).

4.3. Effect of membrane wetting on mass transfer coefficient

Wetting occurs when the liquid solutions enter the pores of the membrane and has been shown to increase the resistance to mass transfer. The ratio of wetting of membrane β can be calculated by Eq. (8). The measured k_m was obtained by the methods described in earlier literature (*Rangwala*, 1996). We

Fig. 8. The plot of $1/K_L$ vs. $X = [(P_{BM}/P_T)(d_i/d_o)]/[H_e v_g^{0.83}]$.

plotted the $1/K_L$ vs. $X = [(P_{BM}/P_T)(d_i/d_o)]/[H_e v_g^{0.83}]$ shown in Fig. 8 ($R^2 = 0.999$) with different PZ and AMP concentrations. Those parameters used here were referred to our previous paper (*Sun et al.*, 2005). The high R^2 indicated the correctness of this method. The linear relationship was obtained and the intercept of the line would be used to calculate the value of k_m . According to the Eq. (8), β could be obtained shown in Table 3. It can be seen that the absorbents containing PZ had higher β value than that using single AMP absorbent. It is probable that PZ was more attractive to PVDF membrane than ethanolamine. It was confirmed by the data of contact angle (Table 3). The β values increased with decreasing contact angle θ except for PZ (Fig. 9(a)). The β values decreased with increasing PZ concentration except for 0.4 PZ. It was because that the viscosity of absorbent increased with PZ concentration shown in Fig. 9(b). The higher liquid viscosity will lead to a lower penetration ratio of liquid into the pore of membrane fiber. But both of the exception mentioned above indicated that the β value resulted from the influences of those factors. So the wetting ratio of membrane was affected not only on the hydrophobicity of membrane but also the affinity between the absorbent and membrane and viscosity of absorbent solution. For the reason to clarify the influence of characteristic of wetting, we tested another alkanolamine MDEA (i.e. *N*-methyldiethanolamine). It was due to its higher viscosity and the calculated β values also listed in Table 3. In comparison of MDEA (1 M) + PZ (0.1 M)

Table 3
Wetting ratio of β at various absorbent in PVDF membrane

C_{AMP} (kmol/m ³)	C_{PZ} (kmol/m ³)	k_m (m/s)	β (%)	μ (m Pa s)	E	θ (°)
1	0.0	7.81×10^{-4}	3.65×10^{-2}	1.1	26.6	90.4
1	0.1	5.00×10^{-4}	6.09×10^{-2}	1.20	64.8	87.5
1	0.2	6.34×10^{-4}	4.19×10^{-2}	1.26	88.3	83.8
1	0.3	7.15×10^{-4}	3.42×10^{-2}	1.32	107	82.6
1	0.4	6.54×10^{-4}	3.50×10^{-2}	1.39	127	79.7
0	0.1	1.09×10^{-4}	3.97×10^{-1}	0.83	64.3	76.5
C_{MDEA} (kmol/m ³)	C_{PZ} (kmol/m ³)	k_m (m/s)	β (%)	μ (m Pa s)	E	θ (°)
1	0.0	7.79×10^{-4}	3.39×10^{-2}	1.2	4	96.3
1	0.1	4.77×10^{-4}	5.91×10^{-2}	1.24	55.8	94.1

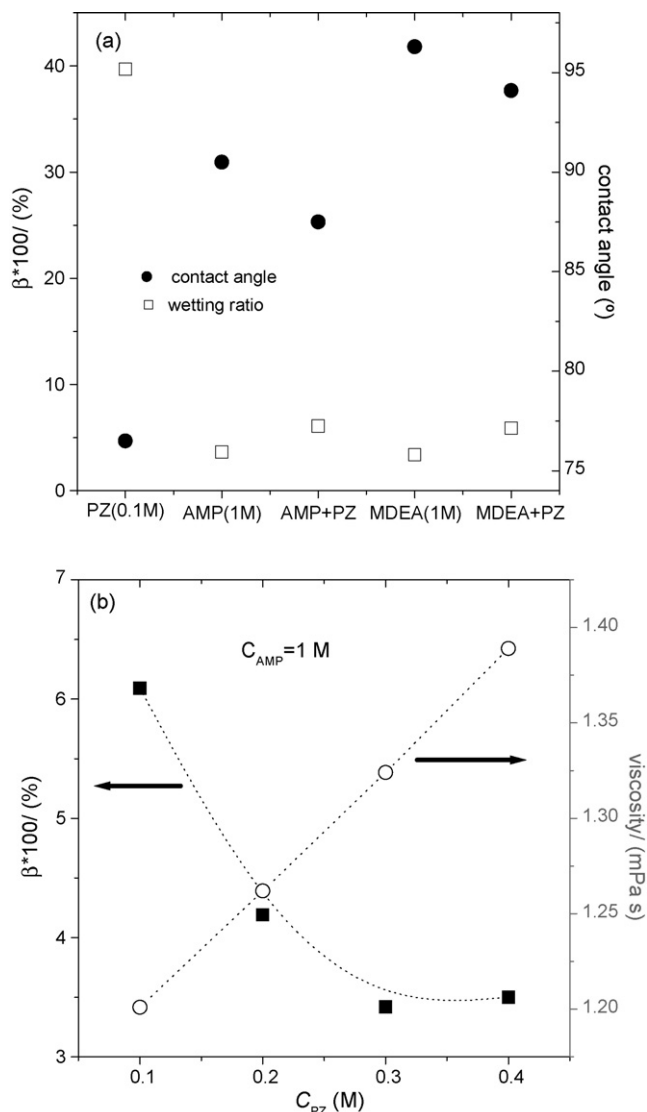


Fig. 9. (a) The β values and viscosities of various absorbents; (b) the β values and contact angle of various absorbents.

with AMP (1 M) + PZ (0.1 M), the former had less wetting ratio than that of the latter. It is due to that the viscosity of MDEA was greater than that of AMP. This phenomenon was also found in the previous report (de Montigny *et al.*, 2006). They examined the CO₂ absorption using aqueous solutions of monoethanolamine (MEA) and AMP with PP and PTFE. They observed that a poorer performance of the PP membranes in AMP solution than that of PP membrane in MEA solution. One possible explanation is PP membrane could be easily wetted by AMP solution.

Compared the β value with other study, Shimada *et al.* (2006) studied the CO₂ absorption using sterically hindered methyl aminoethanol (MAE) in polytetrafluoroethylene (PTFE). They found the liquid penetration into pores of hydrophobic microporous hollow fibers was about 0.06–0.116%. Compared to ours, the lower β value was obtained by us due to the pore size of ours of 0.2 μm was smaller than that of Shimada *et al.* (0.45 μm).

The resistance of membrane diffusion is very important in hollow fiber process. The mass transfer coefficients of

membrane k_m were shown in Table 3. It can be seen that the k_m using different absorbents decreased in the following order of 1 M AMP > 1 M AMP + 0.3 M PZ > 1 M AMP + 0.4 M PZ > 1 M AMP + 0.2 M PZ > 1 M AMP + 0.1 M PZ. This order is a little inconsistent with that of β value. It is because that k_m is not only dependent on the β value but also on the diffusivity of liquid that penetrating into the pore of membrane. The diffusivity of liquid is a function of the viscosity (shown in Table 3). Here the average k_m was 7×10^{-4} m/s ($d_p = 0.2 \mu\text{m}$), it is greater than that by Rangwala (1996) using PP membrane ($k_m = 3\text{--}6.5 \times 10^{-4}$ m/s, $d_p = 0.015 \mu\text{m}$). However, the k_m is smaller than that using PVDF membrane (10×10^{-4} m/s, $d_p = 0.03 \mu\text{m}$), but larger than that using PTFE membrane (5×10^{-4} m/s, $d_p = 1 \mu\text{m}$) by Yeon *et al.* (2003). It is due to the difference of pore sizes and absorbents.

4.4. Analysis of resistance of mass transfer

To compare the resistance of mass transfer in hollow fiber, we express overall resistance as $1/K_L$ in Eq. (2).

The fractional resistance of each step to the overall process can be calculated, e.g., Δ_M in hollow fiber module, by

$$\Delta_M = \frac{R_M}{(R_G + R_M + R_L)} \quad (11)$$

R_M , R_G , and R_L were represented as the resistances of membrane, gas-film and liquid-film diffusion, respectively (i.e. the terms of $(d_i/d_o k_m)(RT/H_c)$, $(d_i/d_o k_g)(1/H_c)$ and $1/Ek_L$). Table 4 showed the calculated mass transfer coefficients and the fractional resistance calculated at various absorbents, flow rates and concentrations. Comparing them, we can find the rate-controlling steps. In this process, the resistance of membrane diffusion was predominated only when single PZ (1 M) and mixed of TEA (1 M) + PZ (0.1 M) as absorbents under the ranges studied. It can be seen that both absorbents had the low CO₂ absorption rates showing in Table 4. The diffusion resistance of gas-film was important as we used the mixed absorbent of AMP and PZ, which increased with increasing the PZ concentration. A high resistance of gas-film diffusion was ever mentioned by Rangwala (1996). He investigated the CO₂ absorption rate using polypropylene (PP) hollow fiber (X-10). In air–CO₂–aq. DEA (0.5 M) system, he found the membrane and gas phase resistance to be 20 and 33.8%. In air–CO₂–aq. NaOH (2 M) system in 0.051 m HFMM, he found the membrane and gas phase resistance to be 35 and 60%. Shimada *et al.* (2006) studied the CO₂ absorption using MAE in polytetrafluoroethylene. They reported that the resistance of membrane diffusion amounted to 76–80% of the total resistance. Here, the AMP (1 M) absorbent had the smallest resistance of membrane diffusion due to its low β value. The resistance of liquid-film diffusion decreased as an increase of the PZ concentration. At the same time, the resistances of gas-film diffusion increased with increasing PZ concentration. It was due to that the enhancement factor (E) increased with

Table 4
The fractional resistances and absorption rate of CO₂ in HFMC

Absorbent	$(1/K_L)_{\text{measured}}$ (m/s)	$1/Ek_L$ (m/s)	$(d_i/d_o k_m)(RT/H_e)$ (m/s)	$(d_i/d_o k_g)(1/H_e)$ (m/s)
PZ (0.1 M)	6913	943	4316	1655
AMP (1 M)	3245	1052	584	1609
TEA (1 M) + PZ (0.1 M)	7019	1913	3313	1793
AMP (1 M) + PZ (0.1 M)	3609	1080	910	1620
AMP (1 M) + PZ (0.2 M)	3161	839	719	1603
AMP (1 M) + PZ (0.3 M)	2985	716	636	1631
AMP (1 M) + PZ (0.4 M)	2954	641	698	1615
MDEA (1 M)	3251	1106	571	1573
MDEA (1 M) + PZ (0.1 M)	3623	1143	892	1587

Absorbent	R (kmol/m ³ s)	Δ_L (%)	Δ_M (%)	Δ_G (%)
PZ (0.1 M)	1.41×10^{-4}	14	62	24
AMP (1 M)	1.98×10^{-4}	32	18	50
TEA (1 M) + PZ (0.1 M)	1.30×10^{-4}	27	47	25
AMP (1 M) + PZ (0.1 M)	2.52×10^{-4}	30	25	45
AMP (1 M) + PZ (0.2 M)	2.88×10^{-4}	26	23	51
AMP (1 M) + PZ (0.3 M)	3.10×10^{-4}	24	21	54
AMP (1 M) + PZ (0.4 M)	3.08×10^{-4}	21	23	54
MDEA (1 M)	0.45×10^{-4}	34	18	48
MDEA (1 M) + PZ (0.1 M)	2.36×10^{-4}	32	25	43

$Q_G = 500$, $Q_L = 200$ (cm³/min).

increasing the PZ concentration. The E values were also listed in Table 3 (Sun et al., 2005).

The fractional resistances at various flow rates were shown in Table 5. It was found that the Δ_G decreased with increasing gas phase flow rates and Δ_L and Δ_M increased with increasing gas phase flow rates. Such results were expected because stagnant-layer of gas would be reduced with increasing gas flow rates.

As mentioned before, the parameter of penetration ratio was important in the resistance of membrane. However, the enhancement factor (E) of absorbents was also significant on the resistance of liquid phase. So the absorption rate of CO₂ with various absorbents in PVDF hollow fiber was also seen in Table 4. As observed in Table 4, the CO₂ absorption rate with blended absorbents was higher than that with single absorbent. Besides, the CO₂ absorption rate using AMP was better than that using TEA. The existence of PZ led to a higher wetting ratio, but it indeed had a higher CO₂ absorption rate. Although, the criteria of absorbent is high reactivity (Li and Chen, 2005), the effects of interaction of absorbent and membrane cannot be neglected.

Table 5
The fractional resistances and absorption rate of CO₂ in HFMC

Q_G (cm ³ /min)	R (kmol/m ³ s)	Δ_L (%)	Δ_M (%)	Δ_G (%)
200	1.70×10^{-4}	19.8	16.7	63.5
250	1.94×10^{-4}	22.2	18.7	59.1
300	2.12×10^{-4}	24.2	20.4	55.2
350	2.29×10^{-4}	25.9	21.8	52.2
400	2.40×10^{-4}	27.4	23.1	49.5
450	2.47×10^{-4}	28.7	24.2	47.0
500	2.52×10^{-4}	29.9	25.2	44.9

$Q_L = 200$ (cm³/min), $C_{AMP} = 1$ M, $C_{PZ} = 0.1$ M.

5. Conclusions

The gas absorption process for removing CO₂ can be carried out in a PVDF hollow fiber membrane contactor system. The CO₂ absorption rate increased with increasing the liquid, gas flow rates and absorbent concentrations. The effective contact areas per volume were influenced by operational flow rate. The effects of viscosity of absorbents and contact angle could not be ignored. The addition of promoter (PZ) not only enhanced the CO₂ absorption rate but also increased the viscosity of absorbent solution. The fractional resistance of membrane diffusion is below 25% by absorbents of AMP and PZ.

Acknowledgement

We thank the National Science Council of the Republic of China for financial support (NSC 95-2221-E-253-016).

References

- Alper, E., "Reaction Mechanism and Kinetics of Aqueous Solutions of 2-Amino-2-methyl-1-propanol and Carbon Dioxide," *Ind. Eng. Chem. Res.*, **29**, 1725 (1990).
- Appl, M., U. Wagner, H. J. Henrici, K. Kuessner, K. Voldamer, and E. Fuerest, "Removal of CO₂ and/or H₂S and/or COS from Gas Containing These Constituents," U.S. Patent, 4, 336, 233 (1982).
- Bishnoi, S. and G. T. Rochelle, "Absorption of Carbon Dioxide into Aqueous Piperazine: Reaction Kinetics, Mass Transfer and Solubility," *Chem. Eng. Sci.*, **55**, 5531 (2000).
- Chakraborty, A. K., G. Astarita, and K. B. Bischoff, "CO₂ Absorption in Aqueous Solutions of Hindered Amines," *Chem. Eng. Sci.*, **41**, 997 (1986).
- Chakravarty, T., U. K. Phukan, and R. H. Weiland, "Reaction of Acid Gases with Mixtures of Amines," *Chem. Eng. Prog.*, **81**, 32 (1985).
- de Montigny, D., P. Tontiwachwuthikul, and A. Chakma, "Using Polypropylene and Polytetrafluoroethylene Membranes in a Membrane Contactor for CO₂ Absorption," *J. Membr. Sci.*, **277**, 99 (2006).

- Desideri, U. and A. Paolucci, "Performance Modeling of a Carbon Dioxide Removal System for Power Plants," *Energy Convers. Manag.*, **40**, 1899 (1999).
- Gabelman, A. and S. T. Hwang, "Hollow Fiber Membrane Contactors," *J. Membr. Sci.*, **159**, 61 (1999).
- Gilliland, E. R. and T. K. Sherwood, "Diffusion of Vapors into Air Streams," *Ind. Eng. Chem.*, **26**, 516 (1934).
- Kreulen, H., C. A. Smolders, G. F. Versteeg, and W. P. M. van Swaaij, "Microporous Hollow Fiber Membranes as Gas-Liquid Contactors. Part 2. Mass Transfer with Chemical Reaction," *J. Membr. Sci.*, **78**, 217 (1993).
- Li, M. H. and Y. C. Lie, "Densities and Viscosities of Solutions Monoethanolamine *N*-Methyldiethanolamine Water and Monoethanolamine 2-Amino-2-methyl-1-propanol Water," *J. Chem. Eng. Data*, **39**, 444 (1994).
- Li, J. L. and B. H. Chen, "Review of CO₂ Absorption Using Chemical Solvents in Hollow Fiber Membrane Contactors," *Sep. Purif. Technol.*, **41**, 109 (2005).
- Nii, S. and H. Takeuchi, "Removal of CO₂ and/or SO₂ from Gas Streams by a Membrane Absorption Method," *Gas Sep. Purif.*, **8**, 107 (1994).
- Rangwala, H. A., "Absorption of Carbon Dioxide into Aqueous Solutions Using Hollow Fiber Membrane Contactors," *J. Membr. Sci.*, **112**, 229 (1996).
- Saha, A. K., S. S. Bandyopadhyay, and A. K. Biswas, "Kinetics of Absorption of CO₂ into Aqueous Solutions of 2-Amino-2-methyl-1-propanol," *Chem. Eng. Sci.*, **50**, 3587 (1995).
- Satori, G. and D. W. Savage, "Sterically Hindered Amines for CO₂ Removal from Gases," *Ind. Eng. Chem. Fundam.*, **22**, 239 (1983).
- Seo, D. J. and W. H. Hong, "Solubilities of Carbon Dioxide in Aqueous Mixtures of Diethanolamine and 2-Amino-2-methyl-1-propanol," *J. Chem. Eng. Data*, **41**, 258 (1996).
- Shimada, K., I. N. Seekkuarachchi, and H. Kumazawa, "Absorption of CO₂ into Aqueous Solutions of Sterically Hindered Methyl Aminoethanol Using a Hydrophobic Microporous Hollow Fiber Contained Contactors," *Chem. Eng. Commun.*, **193**, 38 (2006).
- Song, J. H., S. B. Park, J. H. Yoon, and H. Lee, "Densities and Viscosities of Monoethanolamine + Ethylene Glycol + Water," *J. Chem. Eng. Data*, **41**, 1152 (1996).
- Sun, W. C., C. B. Yong, and M. H. Li, "Kinetics of the Absorption of Carbon Dioxide into Mixed Aqueous Solutions of 2-Amino-2-methyl-1-propanol and Piperazine," *Chem. Eng. Sci.*, **60**, 503 (2005).
- Versteeg, G. F. and W. P. M. van Swaaij, "Solubility and Diffusivity of Acid Gases (CO₂, N₂O) in Aqueous Alkanolamine Solutions," *J. Chem. Eng. Data*, **33**, 29 (1988).
- Wang, R., D. F. Li, and D. T. Liang, "Modeling of CO₂ Capture by Three Typical Amine Solutions in Hollow Fiber Membrane Contactors," *Chem. Eng. Process.*, **43**, 849 (2004).
- Xiao, J., C. W. Li, and M. H. Li, "Kinetics of Absorption of Carbon Dioxide into Aqueous Solutions of 2-Amino-2-methyl-1-propanol + Monoethanolamine," *Chem. Eng. Sci.*, **55**, 161 (2000).
- Xu, G. W., C. F. Zhang, S. J. Qin, W. H. Gao, and H. B. Liu, "Gas-Liquid Equilibrium in CO₂-MDEA-H₂O System and the Effect of Piperazine on It," *Ind. Eng. Chem. Res.*, **37**, 1473 (1998).
- Xu, G. W., C. F. Zhang, S. J. Qin, and Y. H. Wang, "Kinetics Study on Absorption of Carbon Dioxide into Solutions of Activated Methyldiethanolamine," *Ind. Eng. Chem. Res.*, **31**, 921 (1992).
- Yang, M. C. and E. L. Cussler, "Designing Hollow-Fiber Contactors," *AIChE J.*, **32**, 1910 (1986).
- Yeon, S. H., B. Sea, Y. I. Park, K. S. Lee, and K. H. Lee, "Adsorption of Carbon Dioxide Characterized by Using the Absorbent Composed of Piperazine and Triethanolamine," *Sep. Sci. Technol.*, **39**, 3281 (2004).
- Yeon, S. H., B. Sea, Y. I. Park, and K. H. Lee, "Determination of Mass Transfer Rates in PVDF and PTFE Hollow Fiber Membranes for CO₂ Absorptions," *Sep. Sci. Technol.*, **38**, 271 (2003).